

Observation of Quantum Confinement by Strain Gradients

K. Kash, B. P. Van der Gaag, Derek D. Mahoney, A. S. Gozdz, L. T. Florez, and J. P. Harbison
Bellcore, Red Bank, New Jersey 07701-7040

M. D. Sturge

Dartmouth College, Hanover, New Hampshire 03755

(Received 27 November 1990)

We have created one-dimensional quantum wells (quantum wires) by laterally straining a GaAs quantum well with patterned carbon stressors 180 nm in width. We find four well-resolved one-dimensional subbands in the excitation spectra, whose constant spacing of 2.4 meV confirms quantitatively that there is quantum confinement in the parabolic well predicted by continuum elasticity theory. The lateral width of the electron ground state is 35 nm.

PACS numbers: 78.65.Fa, 73.20.Dx

The ability to achieve precise, controlled lateral confinement is the key to the experimental study of a variety of interesting predictions concerning single-particle excitations and collective phenomena in quantum wires and dots [1-4], and is a goal that has been sought by various techniques [5-10]. Strain gradients have been used to accelerate excitons within a semiconductor [11], and to confine electron-hole droplets [12]. We have recently demonstrated that excitons can be confined to quasi-one-dimensional regions by strain patterning of a two-dimensional quantum well [13,14].

We report here the first observation of quantum-wire subbands produced by strain gradients. We use a patterned carbon stressor to generate strain gradients that confine excitons laterally within a GaAs-AlGaAs quantum well, and resolve four quantum-wire subbands, with uniform 2.4-meV splitting, in excitation spectra. The magnitude and uniformity of the observed splitting are in good agreement with the parabolic potential well for electrons calculated using continuum elasticity theory. The lateral width of the electron ground-state wave function is 35 nm. In addition, the observed subband polarization dependence is consistent with a simple model for the electron-hole wave-function overlap.

Details of the fabrication of the strain-confining structures have been discussed elsewhere [15]. Briefly, we use rf plasma deposition employing butane as the carbon-containing gas to put down a 100-nm-thick, uniform layer of amorphous hydrogenated carbon (*a*-C:H) onto a quantum-well sample. In this type of deposition, the resulting stress in the carbon film is produced by bonding defects created by the impact of high-energy ions during growth of the film, and varies in magnitude and sign with the deposition conditions [16,17]. Until the carbon layer is patterned and etched, the semiconductor is undeformed, except for a slight but measurable bowing. Upon etching, the carbon wires expand, and in their partial relaxation they locally deform the underlying quantum well.

Under the conditions used here, the stress in the carbon film is biaxially compressive and of approximate magnitude 500 MPa. The quantum-well sample was grown by

molecular-beam epitaxy in the following sequence: 500 nm of GaAs, a 200-nm lower barrier layer consisting of 160 nm of $\text{Al}_{0.3}\text{Ga}_{0.7}\text{As}$ followed by a twenty-layer superlattice of 1.4 nm of GaAs and 0.6 nm of AlAs, inserted to smooth the lower interface and to trap any impurities from entering the quantum well, the 12-nm GaAs quantum well, a 20-nm barrier of $\text{Al}_{0.3}\text{Ga}_{0.7}\text{As}$, and a 30-nm GaAs cap layer. The carbon layer was patterned and etched to form 40- μm square arrays of stressor wires of 180-nm width on 600-nm centers. The region of maximum volume dilation in the well occurs under the center of the wire, and compressively stressed shoulders appear at the edges of the wire, as shown in Fig. 1(a) in the calculated contour plot. At the center, the strain-induced band-gap shrinkage forms the exciton potential well. The calculated strain tensor in the plane of the center of the quantum well is shown in Fig. 1(b).

Luminescence and excitation spectra for a sample temperature of 10 K are shown in Fig. 2 both for an unpatterned region of the sample and for an adjacent array of 180-nm-wide wires. The luminescence spectrum of the wire-patterned region exhibits a redshift of 22 meV with respect to that of the unpatterned region. This redshift is a direct measure of the depth of the exciton potential

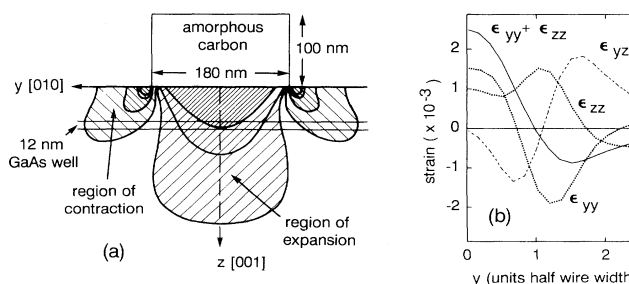


FIG. 1. (a) Cross section, to scale, of a wire-patterned region of the sample, showing the amorphous carbon stressor and the underlying 12-nm GaAs well. A contour plot of the volume dilation is superimposed. The potential well for excitons lies under the center of the carbon wire. (b) Nonzero components of the strain tensor in the plane of the quantum well, calculated by continuum elasticity theory as described in the text.

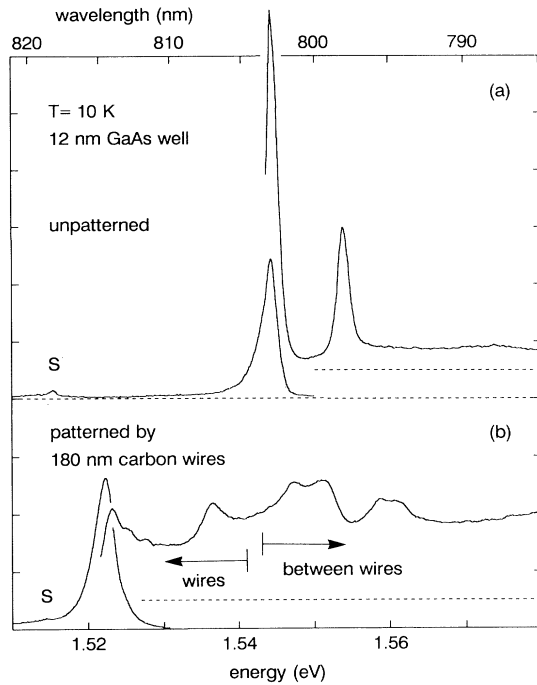


FIG. 2. Photoluminescence and excitation spectra of two regions of the quantum well. The horizontal dashed lines indicate zeros. (a) Unpatterned region, with a heavy-hole exciton peak of 1.5-meV linewidth and a Stokes shift of 0.2 meV; (b) adjacent region, patterned by an array of 180-nm-wide carbon wires on 600-nm centers. The portion of the excitation spectrum below 1.543 eV arises from absorption within the strain-induced wire. The lower of the two peaks associated with wire-confined excitons is Stokes shifted by 0.8 meV from the luminescence peak, and shows splitting into quantum-wire subbands. The two excitation spectra are shown on the same vertical scale. Luminescence peaks from the GaAs substrate are labeled S.

well. In the excitation spectrum of the unpatterned region of the well, the heavy-hole peak is 1.5 meV in width, and has a small Stokes shift of 0.2 meV. The excitation spectrum of the patterned region is shown on the same vertical scale. At energies above 1.543 eV this spectrum shows light- and heavy-hole exciton peaks arising from absorption in the regions of the well between the wires. These peaks are split, broadened, and blueshifted by the laterally modulated compressive stress generated between the wires (see Fig. 1). This interpretation is confirmed by the dependence of the relative intensities of these peaks on the spacing of the wires, not shown here. Excitons created between the wires are within a diffusion length of the lateral potential wells, and consequently are trapped and recombine within the wirelike potential wells. The longer-wavelength portion of the excitation spectrum shows two main exciton peaks arising from the redshifted band gap in the wirelike lateral potential wells. These two main peaks are associated with the two valence subband edges. The lower-energy peak is Stokes shifted from the luminescence peak by 0.8 meV. This larger Stokes shift is presumably a result of inhomogeneous

broadening of the exciton peak by wire-width fluctuations. This lowest-energy wire-confined exciton peak shows a structure arising from the strain-induced lateral confinement, seen in closer detail in the polarized excitation spectra of Fig. 3. Four quantum-wire subbands, with uniform spacings of 2.4 ± 0.2 meV, are resolved in both polarizations. Subband structure is not resolved for the higher-lying exciton peak, perhaps as a result of greater inhomogeneous broadening for this exciton.

In order to calculate the strain-induced lateral potential wells for electrons and holes in this structure, we first calculate the strain tensor in the plane of the well [Fig. 1(b)]. Because the characteristic dimensions are large compared to atomic spacing, continuum elasticity theory applies. We use here, as previously, a standard finite-element approach [15,18]. The anisotropic elastic coefficients of GaAs are used throughout the semiconductor structure [19]. A Young's modulus of 3.59×10^7 MPa and a Poisson ratio of 0.3 are used for the isotropic carbon layer [16].

Application of the strain Hamiltonian [19-24] yields the strain modulation of the band edges shown in Fig. 4. The *s*-like conduction-band edge is sensitive only to the hydrostatic, or volume, dilation. The *p*-like valence-band edges are strongly modulated and mixed by the shear-

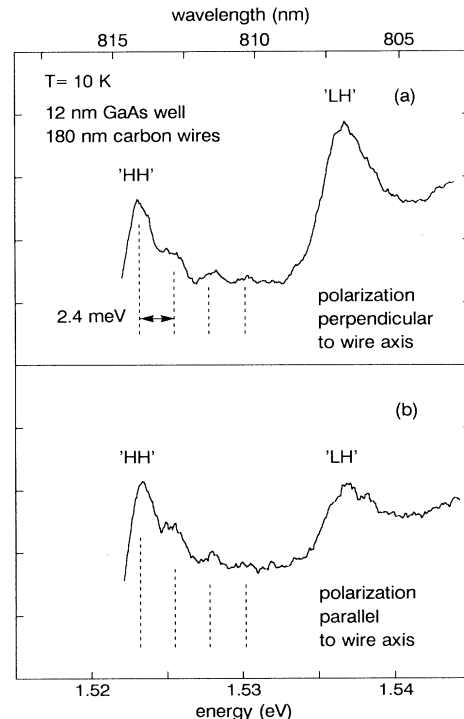


FIG. 3. (a),(b) Polarized excitation spectra of the quantum-wire exciton peaks. The two main peaks are labeled LH and HH, although the two valence subband edges are strongly mixed by the anisotropic strain. Four quantum-wire subbands, evenly spaced by 2.4 ± 0.2 meV, are clearly resolved in the HH transitions, for both polarizations. The intensity scales of the two spectra are the same.

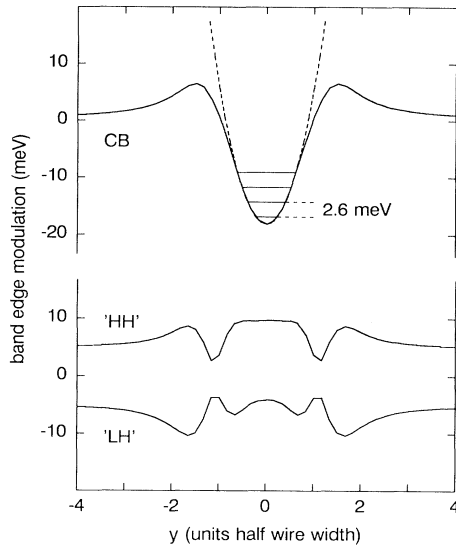


FIG. 4. Calculated lateral variation of the conduction- and valence-band edges. The four lowest quantum-wire subbands of the nearly parabolic confinement potential are shown. The calculated subband spacing of 2.6 meV is in good agreement with the data of Fig. 3. Note that both electrons and heavy holes are confined to the region under the wire.

strain components. Because the wire axis and the normal to the quantum well are oriented along [100] crystallographic directions, piezoelectric fields along the y axis are zero by symmetry, and so do not affect the confinement potential [25]. We have scaled the strain tensor of Fig. 1(b) to obtain agreement with the observed redshift of the band gap. This scaling is in agreement with a bowing measurement of the strain produced by the planar carbon layer [26]. We obtain at the center of the wire a nearly parabolic potential well for electrons of 18-meV depth, relative to the unstrained band edge, with potential barriers located near the edges of the stressors. From the calculated curvature and use of an electron mass of $0.067m_0$ we calculate a subband splitting of 2.6 meV. We find a smaller, wider potential well of approximately 5 meV for the highest-lying hole band edge, with a curvature at the wire center that is an order of magnitude smaller than that of the electron. We emphasize that this formation of the hole potential well at the center of the structure is not a general result of strain patterning [23].

In considering the lateral confinement of the exciton, we note the analogy to the case of quantum-well systems with small valence-band offsets, as is found to occur for certain II-VI material systems [27]. With an exciton binding energy of 7.5 meV for the unstrained well and an in-plane exciton radius of 13 nm [28,29], this is a situation in which the electron is confined laterally by the strain-induced potential well, and the hole is confined laterally by its Coulomb attraction to the electron. A very weak dependence of the exciton binding energy on the well width is found in the quantum-well case, and may be

assumed here as well [29]. Thus, the exciton subband splitting that we observe is determined by the electron confinement. Our calculated energy-level splitting of 2.6 meV is in very good agreement with our observed splitting of 2.4 ± 0.2 meV. The lateral width of the ground-state electron wave function, given by the full width at half maximum of the probability density, is 35 nm. We emphasize that this lateral electron confinement is achieved with a relatively wide (180 nm) carbon wire and a relatively small electron confinement potential of 18 meV. We further note that since the energy-level separation for the parabolic lateral well is proportional to the square root of the curvature of this well, we expect for larger wires that the peak splittings should scale as the inverse of the wire width and as the square root of the depth of the lateral potential well. For 380-nm-wide stressor wires, we observe 1.5-meV peak splittings in luminescence and excitation spectra. These larger wires produce, as expected [23], a somewhat deeper lateral potential well than do the smaller wires (33-meV redshift in luminescence, rather than 22 meV). Thus, we find that the experimentally observed energy-level separations vary as expected with the size of the wire.

We now focus on the observed polarization dependence of the wire-confined exciton absorption of Fig. 3. The entire portion of the spectrum associated with transitions from the heavy-hole (HH) subband is approximately 25% stronger in absorption for polarization parallel to the wire axis than for the perpendicular polarization. The light-hole (LH) peak oscillator strength is approximately equal to that of the HH peak for polarization perpendicular to the wire axis, and approximately 40% of that of the HH peak for the parallel polarization. As shown in Fig. 1, the shear strain at the center of the wire is spatially quite uniform over an exciton diameter. The polarization anisotropy to be expected here for the various subbands observed is thus a particularly simple case, determined by the heavy- and light-hole mixing by the uniform uniaxial strain at the center of the wire [30]. Thus, in contrast to the case in which lateral confinement of the hole determines hole subband mixing [31], we expect, and indeed, within our experimental uncertainty, observe in Fig. 3, that the polarization anisotropy is independent of subband index.

In considering calculation of the relative oscillator strengths of the quantum-wire subbands, we note that accurate calculation requires inclusion of finite- k terms in the exciton wave function [32–34]. However, in light of the result that inclusion of such terms only qualitatively explains the observed oscillator strengths in the much more extensively studied case of quantum-well subbands [34], an accurate calculation for the present case would be extremely complex, and we leave it to future work.

In summary, we have achieved lateral quantum confinement of excitons with strain gradients. Using carbon stressors, we have produced lateral, parabolic potential wells that confine the electron ground state to a wire of

effective width 35 nm. The spacing of 2.4 meV for the four resolved subbands agrees well with our calculated value of 2.6 meV based upon continuum elasticity theory, and the observed polarization dependence of the oscillator strengths is consistent with a simple model incorporating strain-induced valence-band mixing. Strain patterning has certain important advantages, specifically the flexibility in patterning of potential wells, the lack of free surfaces for carriers to interact with, and the absence of constraints imposed by considerations of crystal growth. These advantages make possible a variety of fundamental experiments concerning optical interactions with single-particle and collective excitations in quantum wires and dots.

We are grateful to I-Hsing Tan for pointing out an error in our calculation of the band-edge modulation in Ref. [23]. We also gratefully acknowledge valuable discussions with J. M. Worlock in the initial phases of this work. This work was partially supported by the U.S. Office of Naval Research under Grant No. N0014 91J1429.

- [1] H. Sakaki, K. Wagatsuma, J. Hamasaki, and S. Saito, *Thin Solid Films* **36**, 497 (1976).
- [2] E. Hanamura, *Phys. Rev. B* **37**, 1273 (1988).
- [3] G. W. Bryant, *Phys. Rev. B* **37**, 8763 (1988).
- [4] L. Banyai, Y. Z. Hu, M. Lindberg, and S. W. Koch, *Phys. Rev. B* **38**, 8142 (1988).
- [5] M. Kohl, D. Heitmann, P. Grambow, and K. Ploog, *Phys. Rev. Lett.* **63**, 2124 (1989).
- [6] E. Kapon, D. M. Hwang, and R. Bhat, *Phys. Rev. Lett.* **63**, 430 (1989).
- [7] M. Tsuchiya, J. M. Gaines, R. H. Yan, R. J. Simes, P. O. Holtz, L. A. Coldren, and P. M. Petroff, *Phys. Rev. Lett.* **62**, 466 (1989).
- [8] Y. Hirayama, Y. Suzuki, S. Tarucha, and H. Okamoto, *Jpn. J. Appl. Phys.* **24**, L516 (1985).
- [9] J. Cibert, P. M. Petroff, G. J. Dolan, D. J. Werder, S. J. Pearton, A. C. Gossard, and J. H. English, *Appl. Phys. Lett.* **49**, 1275 (1986).
- [10] H. M. Cox, D. E. Aspnes, S. J. Allen, P. Bastos, D. M. Hwang, S. Mahajan, M. A. Shahid, and P. C. Morais, *Appl. Phys. Lett.* **57**, 611 (1990).
- [11] V. S. Bagaev, T. I. Galkina, O. V. Gogolin, and L. V. Keldysh, *Pis'ma Zh. Eksp. Teor. Fiz.* **10**, 309 (1969) [*JETP Lett.* **10**, 195 (1969)].
- [12] J. P. Wolfe, R. S. Markiewicz, C. Kittel, and C. D. Jeffries, *Phys. Rev. Lett.* **34**, 1292 (1975).
- [13] K. Kash, J. M. Worlock, M. D. Sturge, P. Grabbe, J. P. Harbison, A. Scherer, and P. S. D. Lin, *Appl. Phys. Lett.* **53**, 782 (1988).
- [14] The achievement of strong quantum confinement of excitons by strain gradients was recently claimed in D. Gershoni, J. S. Weiner, S. N. G. Chu, G. A. Baraff, J. M. Vandenberg, L. N. Pfeiffer, K. West, R. A. Logan, and T. Tanbun-Ek, *Phys. Rev. Lett.* **65**, 1631 (1990). Our calculation of the strain tensor for that system shows that strain confinement cannot be occurring in that case [K. Kash, Derek D. Mahoney, and H. M. Cox, *Phys. Rev. Lett.* **66**, 1374 (1991)].
- [15] K. Kash, J. M. Worlock, Derek D. Mahoney, A. S. Gozdz, B. P. Van der Gaag, J. P. Harbison, P. S. D. Lin, and L. T. Florez, *Surf. Sci.* **228**, 415 (1990).
- [16] D. Nir, *Thin Solid Films* **146**, 27 (1987).
- [17] John C. Angus, Peter Koidl, and Stanley Domitz, in *Plasma Deposited Thin Films*, edited by J. Mort and F. Jansen (CRC, Boca Raton, FL, 1986), p. 89.
- [18] Klaus-Juergen Bathe and Edward L. Wilson, *Numerical Methods in Finite Element Analysis* (Prentice-Hall, Englewood Cliffs, NJ, 1976).
- [19] *Physics of Group IV Elements and III-V Compounds*, edited by O. Madelung, Landolt-Börnstein, New Series, Group III, Vol. 17, Pt. a (Springer-Verlag, Berlin, 1982).
- [20] G. E. Pikus and G. L. Bir, *Fiz. Tverd. Tela* **1**, 1642 (1959) [*Sov. Phys. Solid State* **1**, 136 (1959)].
- [21] W. H. Kleiner and L. M. Roth, *Phys. Rev. Lett.* **2**, 334 (1959).
- [22] Thomas H. Bahder, *Phys. Rev. B* **41**, 11992 (1990).
- [23] K. Kash, B. P. Van der Gaag, J. M. Worlock, A. S. Gozdz, D. D. Mahoney, J. P. Harbison, and L. T. Florez, in *Localization and Confinement of Electrons in Semiconductors*, Springer Series in Solid State Sciences Vol. 97 (Springer-Verlag, Berlin, 1990).
- [24] The valence-band-edge modulation is $\delta E_{\pm} = a(\epsilon_{yy} + \epsilon_{zz}) \pm (a^2 + \beta^2 + \gamma^2)^{1/2}$, where $a = \frac{1}{2}A + b(\frac{1}{2}\epsilon_{yy} - \epsilon_{zz})$, $\beta = \frac{1}{2}\sqrt{3}b\epsilon_{yy}$, and $\gamma = d\epsilon_{yz}$, for the wire axis oriented along x . A is the splitting of the light and heavy holes. The values of 1.1, -2 , and -5 eV are used for the Pikus-Bir hydrostatic deformation potential a and shear deformation potentials b and d . This equation corrects an error made in Ref. [23] for the valence-band modulation.
- [25] J. F. Nye, *Physical Properties of Crystals* (Clarendon, Oxford, 1985), p. 122.
- [26] D. S. Campbell, in *Handbook of Thin Film Technology*, edited by L. I. Maissel and R. Glang (McGraw-Hill, New York, 1970), Chap. 12.
- [27] Ji-Wei Wu and A. V. Nurmikko, *Phys. Rev. B* **38**, 1504 (1988).
- [28] G. Bastard, E. E. Mendez, L. L. Chang, and L. Esaki, *Phys. Rev. B* **26**, 1974 (1982).
- [29] Ronald L. Greene and K. K. Bajaj, *Solid State Commun.* **45**, 831 (1983).
- [30] K. Kash, J. M. Worlock, A. S. Gozdz, B. P. Van der Gaag, J. P. Harbison, P. S. D. Lin, and L. T. Florez, *Surf. Sci.* **229**, 245 (1990).
- [31] P. C. Sercel and K. J. Vahala, *Appl. Phys. Lett.* **57**, 545 (1990).
- [32] G. D. Sanders and Y. C. Chang, *Phys. Rev. B* **32**, 5517 (1985).
- [33] Bangfen Zhu, *Phys. Rev. B* **37**, 4689 (1988).
- [34] W. T. Masselink, P. J. Pearah, J. Klem, C. K. Peng, H. Morkoc, G. D. Sanders, and Y. C. Chang, *Phys. Rev. B* **32**, 8027 (1985).